

Adaptive and Robust Control of DFIG-Based Wind Energy Conversion System Using Fuzzy Logic

1st Choug Noredine

Electrical Engineering Laboratory (LGE), Electrical Engineering Department, Faculty of Technology, University of M'Sila, University Pole, Road Bordj Bou Arreridj M'sila 28000, Algeria.
choug.noredine@univ-msila.dz

2nd fegriche abderahmane

Electrical Engineering Laboratory (LGE), Electrical Engineering Department, Faculty of Technology, University of M'Sila, University Pole, Road Bordj Bou Arreridj M'sila 28000, Algeria.
abderahmane.fegriche@univ-msila.dz

Abstract—

the objective of this work is to optimize the performance of a wind energy conversion system (WECS) based on a Doubly-Fed Induction Generator (DFIG). A vector control strategy based on stator flux orientation is implemented to independently regulate the active and reactive power exchanged between the stator and the grid. three innovative controllers are proposed and compared: a fuzzy logic controller (FLC) and a Proportional-Integral controller with Adaptive Fuzzy Gain Scheduling (AFGPI). The latter adjusts its gains in real time using a fuzzy algorithm based on the error and its derivative, thereby improving the system's dynamic response. Simulations performed in MATLAB/Simulink on a 1.5 MW DFIG model validate the effectiveness of both approaches, with the AFGPI showing particular robustness against wind speed variations and grid disturbances. The results highlight a clear advantage in terms of dynamic performance and stability compared to conventional control methods.

Keywords— WECS; Vector control; PI controle; fuzzy logic controller; PI-fuzzy controller.

Introduction

Sustainable development and the growing demand for clean energy have increasingly drawn the attention of researchers toward renewable energy sources. Among these, wind energy stands out as a key area of technological innovation and investment. As a clean, abundant, and greenhouse gas-free resource [1–3], wind power is becoming a major contributor to the global energy mix. Currently, variable-speed wind turbine systems with power ratings exceeding 1 MW are commonly deployed, especially to optimize energy extraction in large-scale wind farms.

Doubly-Fed Induction Generators (DFIGs) are widely used in such systems due to their numerous advantages [4–7], including variable-speed operation ($\pm 30\%$ around synchronous speed), decoupled control of active and reactive power, lower acoustic noise, and reduced mechanical losses compared to other generator types [8–11].

This paper focuses on the control of electrical power exchanged between the DFIG stator and the grid by

independently regulating active and reactive power. In recent years, advanced control strategies have emerged that are more competitive and better suited to handle system nonlinearities and robustness challenges. Among these, fuzzy logic has proven to be a promising alternative.

After modeling the complete wind energy conversion system, two control strategies are developed and compared: a conventional fuzzy logic controller (FLC) and a Proportional-Integral controller with Adaptive Fuzzy Gain Scheduling (AFGPI).

The paper is structured as follows: Section 1 presents the modeling of the DFIG-based WECS; Section 2 outlines the active and reactive power control strategy; Section 3 describes the controller design and provides performance comparisons. Simulation results and analysis are discussed in Section 4, followed by conclusions in Section 5

I. MODELING WIND ENERGY CONVERSION SYSTEMS

The wind energy conversion system comprises a wind turbine that drives the DFIG through a variable-speed gearbox. The stator is directly connected to the electrical grid, while the rotor is interfaced with the grid through a back-to-back converter configuration, consisting of two bidirectional static converters linked by a DC bus, as illustrated in Fig. 1 [11–13].

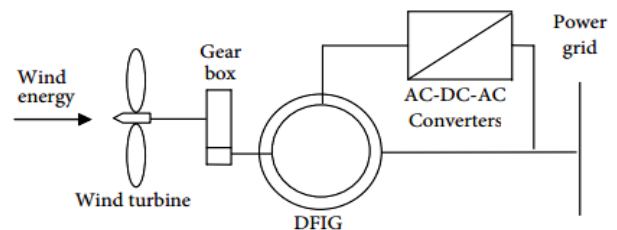


Fig. 1. Variable Speed Wind Turbine with DFIG

A. WIND MODELING

A deterministic model of wind speed uses a sum of harmonics [14].

$$V_v(t) = A + \sum_{n=1}^i (a_n \sin(b_n w_v f)) \quad (1)$$

with: A is constant, a_n, b_n, w_v and, represent respectively the amplitude and the pulsation of the wind sample.

From equation 1 we can note:

$$V_v(t) = 8 + 0.4 \sin(1.47t) + 2 \sin(0.56665t) + \sin(5.75t) + 0.8 \sin(4.266t) \quad (2)$$

B. TURBINE MODELING

he rotation of the turbine blades is driven by the wind speed V_v , resulting in the generation of aerodynamic power P_{aero} on the turbine shaft [15]. This power can be calculated using equation (3):

$$P_{aero} = \frac{1}{2} \rho \pi R^2 V_v^3 C_p(\lambda, \beta) \quad (3)$$

Where, ρ is the air density (kg/m^3), R is the blade radius (m), C_p is the performance coefficient of the turbine called also aerodynamic efficiency of the wind turbine which is a function of the pitch angle of rotor blades β (degrees) and λ the tip-speed ratio, V_v is the wind speed in (m/s).

where:

ρ : air density (kg/m^3)

R : blade radius (m)

V_v : wind speed (m/s)

$C_p(\lambda, \beta)$: Turbine performance coefficient (aerodynamic efficiency), a function of the tip-speed ratio (λ) and the blade pitch angle (β) (degrees).

The tip-speed ratio λ is expressed as follows

$$\lambda = \frac{\Omega_{turb} R}{V_v} \quad (4)$$

For a wind turbine of 1.5 MW, [7] give the expression of the power coefficient:

$$C_p(\lambda, \beta) = (0.5 - 0.167(\beta - 2)) \sin\left(\frac{\pi(\lambda + 0.1)}{10 - 0.3\beta}\right) - 0.00184(\lambda - 3)(\beta - 2) \quad (5)$$

The aerodynamic torque is expressed as follows [13]:

$$T_{aero} = \frac{1}{2\Omega} \rho \pi R^2 V_v^3 C_p(\lambda, \beta) \quad (6)$$

The role of the gearbox is to adapt the slow speed of the turbine to the fast speed of the generator and the aerodynamic torque to the mechanical torque according to the following equations:

$$T_g = \frac{T_{aero}}{G} \quad (7)$$

$$\Omega_{turb} = \frac{\Omega_{mec}}{G} \quad (8)$$

The mechanical equations of the system can be characterized by:

$$J_T \frac{d\Omega_{mec}}{dt} = T_{mec} = T_g - T_{em} - f\Omega_{mec} \quad (9)$$

$$\text{With: } J_T = \frac{J_{turb}}{G^2} + J_g$$

Where T_g the torque of the generator, $\Omega_{mec}, \Omega_{turb}$ are speed of the generator and turbine, J_T is total inertia, J_g is the

generator inertia, and J_{turb} is the Turbine inertia, f is the viscous friction coefficient.

Keep your text and graphic files separate until after the text has been formatted and styled. Do not use hard tabs, and limit use of hard returns to only one return at the end of a paragraph. Do not add any kind of pagination anywhere in the paper. Do not number text heads-the template will do that for you.

C. MODELING OF THE DFIG

The DFIG model, represented in the d-q Park reference frame, is described by the following equations [11].

$$\begin{cases} V_{sd} = R_s I_{sd} + \frac{d\varphi_{sd}}{dt} - \omega_s \varphi_{sq} \\ V_{sq} = R_s I_{sq} + \frac{d\varphi_{sq}}{dt} + \omega_s \varphi_{sd} \\ V_{rd} = R_r I_{rd} + \frac{d\varphi_{rd}}{dt} - \omega_r \varphi_{rq} \\ V_{rq} = R_r I_{rq} + \frac{d\varphi_{rq}}{dt} + \omega_r \varphi_{rd} \end{cases} \quad (10)$$

The stator and rotor flux can be expressed as:

$$\begin{cases} \varphi_{sd} = L_s I_{sd} + M I_{rd} \\ \varphi_{sq} = L_s I_{sq} + M I_{rq} \\ \varphi_{rd} = L_r I_{rd} + M I_{sd} \\ \varphi_{rq} = L_r I_{rq} + M I_{sq} \end{cases} \quad (11)$$

Where

s, r are stator and rotor subscripts, $V_{sd}, V_{sq}, V_{rd}, V_{rq}$ are respectively the direct and quadrate stator and rotor voltages, $I_{sd}, I_{sq}, I_{rd}, I_{rq}$ are respectively the direct and quadrate stator and rotor currents, $\varphi_{sd}, \varphi_{sq}, \varphi_{rd}, \varphi_{rq}$ are respectively the direct and quadrate stator and rotor fluxes, L_s, L_r, M stator and rotor per phase winding and magnetizing inductances, P is the pair pole number, R_s and R_r are the stator and rotor phase resistances respectively, ω_s, ω_r are respectively the synchronous angular speed of the generator and the angular speed of the rotor.

The electromagnetic torque is expressed in terms of currents and fluxes by:

$$T_{em} = p \frac{M}{L_s} (I_{rq} \varphi_{sd} - I_{rd} \varphi_{sq}) \quad (12)$$

II. ACTIVE AND REACTIVE POWER CONTROL STRATEGIES FOR DFIG

The equations are an exception to the prescribed specifications of this template. You will need to determine whether or not your equation should be typed using either the Times New Roman or the Symbol font (please no other font). To create multileveled equations, it may be necessary to treat the equation as a graphic and insert it into the text after your paper is styled.

In steady-state operation, with the q-axis of the synchronous rotating reference frame aligned with the stator flux vector, the system's behavior is described by the following equations:

$$\varphi_{sd} = \varphi_s, \varphi_{sq} = 0$$

The electromagnetic torque of equation (12) is then written as follows

$$T_{em} = p \frac{M}{L_s} (I_{rq} \varphi_{sd}) \quad (13)$$

With a stable grid voltage V_s , the stator flux φ_s remains constant. Under this condition, and based on equation 13, the electromagnetic torque becomes solely dependent on the q-axis component of the rotor current. For medium to high-power wind turbine generators, the stator resistance R_r is typically negligible [7, 10, 17].

The Stator voltage and flux can be simplified as:

$$\begin{cases} V_{sd} = 0 \\ V_{sq} = V_s = \omega_s \varphi_s \\ \varphi_{sd} = L_s I_{sd} + M I_{rd} \\ 0 = L_s I_{sq} + M I_{rq} \end{cases} \quad (14)$$

The stator active and reactive power and rotor voltage are written as follows:

$$\begin{cases} P_s = -V_s \frac{M}{L_s} I_{rq} \\ Q_s = \frac{V_s^2}{L_s \omega_s} - V_s \frac{M}{L_s} I_{rd} \end{cases} \quad (15)$$

$$\begin{cases} V_{rd} = R_r I_{rd} - g \omega_s L_r \sigma I_{rq} \\ V_{rq} = R_r I_{rq} + g \omega_s L_r \sigma I_{rd} + g \frac{M V_s}{L_s} \end{cases} \quad (16)$$

$$\text{With: } \sigma = \frac{\omega_s - \omega}{\omega_s}, \sigma = 1 - \frac{M^2}{L_s L_r}$$

Where: g is the slip and σ is the leakage factor.

The preceding equations allow establishing a block diagram of the electrical system to be regulated given by the Fig. 2:

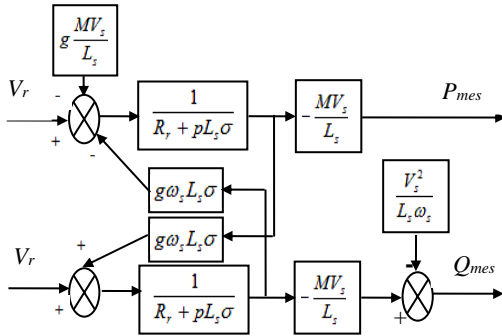


Fig. 2. Block diagram of the system to be regulated.

III. CONTROLLERS SYNTHESIS

A. SYNTHESIS OF PI CONTROLLER

The block diagram of the PI controller system is presented in Figure 3

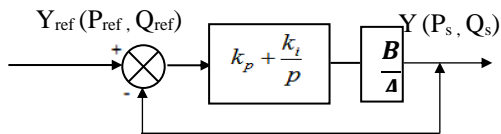


Fig. 3. PI Controller Design for Power Systems

With:

$$A = L_s R_s + p L_s L_r \sigma, B = M V_s$$

The open loop transfer function $G(p)$ is given by:

$$G(p) = \frac{p + \frac{k_i}{k_p}}{\frac{p}{k_p}} \cdot \frac{\frac{M V_s}{L_s L_r \sigma}}{p + \frac{R_r}{L_r \sigma}} \quad (17)$$

We use the method of poles compensation for the synthesis of the Controller in order to eliminate the zero present on the transfer function, which results in the following equality:

$$\frac{k_i}{k_p} = \frac{R_r}{L_r \sigma} \quad (18)$$

Thus the closed-loop transfer function $G(p)$ can be expressed by:

$$G(p) = \frac{1}{1 + \tau p} \quad (19)$$

$$\text{With } \tau = \frac{L_s L_r \sigma}{k_p M V_s}$$

$$\begin{cases} k_p = \frac{\sigma L_s L_r}{\tau M V_s} \\ k_i = \frac{L_s R_r}{\tau M V_s} \end{cases} \quad (20)$$

B. FUZZY CONTROLLER FOR POWER SYSTEM.

The proposed control system utilizes two independent, conventional fuzzy logic controllers (FLCs) for the regulation of stator active and reactive powers (P_s, Q_s) in the DFIG. The FLCs generate the necessary rotor voltage references. The design methodology, comprised of three primary steps, is presented in Fig 4

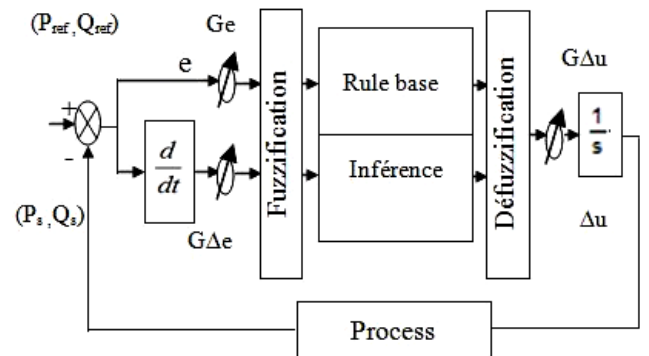


Fig. 4. Fuzzy Logic Control of Active and Reactive Power

In the diagram above, the FLC inputs are calculated at time k as follows:

e : Error, it is defined by:

$$e(k) = (P_{sref}, Q_{sref})(k) - (P_s, Q_s)(k) \quad (18)$$

Δe : The derivative of the error it is approximated by:

$$\Delta e(k) = \frac{e(k) - e(k-1)}{T_e} \quad (19)$$

T_e : is the sampling period.

The output of the regulator is given by:

$$V_{r,dq}(k) = V_{r,dq}(k-1) + \Delta u(k) \quad (20)$$

The gains G_e , $G_{\Delta e}$, and $G_{\Delta u}$ are the gains that allow changing the sensitivity of the fuzzy regulator without changing the fuzzy structure. They are used to transform the physical values of the inputs into a normalized domain $[-1 \ 1]$ called discourse universe.

For the membership functions, we chose for each variable the triangular and trapezoidal shapes as shown in Fig. 5.

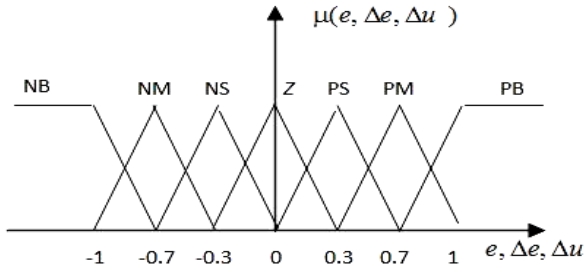


Fig. 5. Membership functions for input variables, e , Δe and output Δu .

To simplify the description of the inferences, we use an inference matrix, see Table 1

TABLE I. BASIC CONTROL OF ACTIVE AND REACTIVE POWER

$e, \Delta e$	NB	NM	NS	Z	PS	PM	PB
NB	NB	NB	NB	NB	NM	NP	Z
NM	NB	NB	NB	NM	NS	Z	PS
NS	NB	NB	NM	NS	Z	PS	PM
Z	NB	NM	NS	Z	PS	PM	PB
PS	NM	NS	Z	PS	PM	PB	PB
PM	NS	Z	PS	PM	PB	PB	PB
PB	Z	PP	PM	PB	PB	PB	PB

The inference method used is the method (Max-Min) which is easy to implement.

For defuzzification, we use the center of gravity method to obtain [5]:

$$dV_{r,dq} = \frac{\sum_{i=1}^m u(dV_{r,dq})dt}{\sum_{i=1}^m u(dV_{r,dq})} \quad (21)$$

C. PI CONTROL WITH ADAPTIVE FUZZY GAIN

The proportional-integral (PI) controller is a linear control system favored in mechanical operations for its simple design, ease of implementation, and satisfactory performance. However, the field of adaptive control has seen considerable progress recently, leading to the integration of artificial intelligence into PI control strategies. This integration aims to enhance performance and tackle a wider array of control issues. The availability of faster computing resources and larger memory capacities has enabled the practical implementation of these high-performance adaptive algorithms [20, 21-22]. In the time domain, a classical PI controller can be defined as follows:

$$u(t) = K_p e(t) + K_i \int_0^t e(t) dt \quad (22)$$

The fuzzy controller fine-tunes the parameters of the pi controller and produces fresh parameters tailored to varying operational conditions. this is accomplished by taking into account the error and its derivative as inputs. fig 6 illustrates the block diagram of the adaptable fuzzy gain for the pi controller

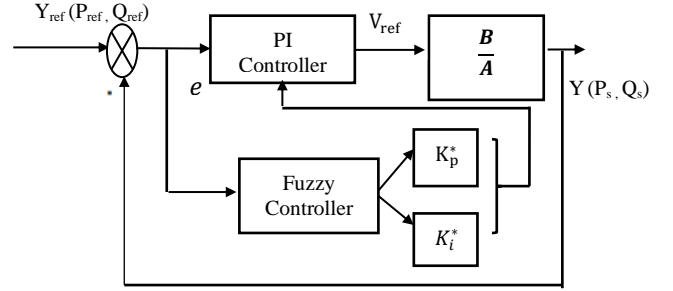


Fig. 6. PI Controller with Adaptive Fuzzy Gain

We use the method of poles compensation for the synthesis of the Controller in order to eliminate the zero present on the transfer function, which results in the following equality

The inputs of the FLC fuzzy controller are: error (e) and the derivative of the error (Δe) the outputs are: the normalized value of the proportional action K_p^* and the normalized value of the integral action K_i^* .

the normalization pi parameters are given by [22]:

$$\begin{cases} K_p^* = \frac{K_p - K_{pmin}}{K_{pmax} - K_{pmin}} \\ K_i^* = \frac{K_i - K_{imin}}{K_{imax} - K_{imin}} \end{cases}$$

The inputs of fuzzy controller are: error (e) and derivative (Δe) of error are designed as in fig 7

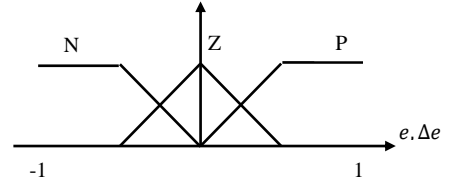


Fig. 7. Membership functions the inputs (e) and Δe

The membership functions the outputs K_p^* and K_i^* gain of the active and reactive powers controller are designed as in fig. 8, fig. 9. which: negative noted n; zero noted z; positive noted ; positive small noted PS; positive medium noted MP; positive big noted PB.

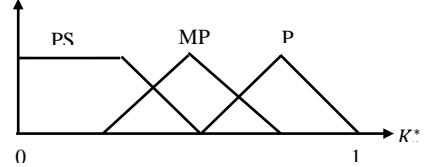


Fig. 8. Membership functions the output K_p^*

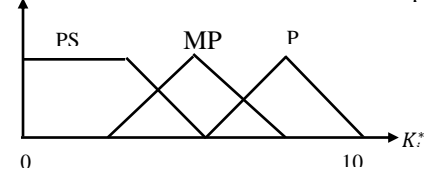


Fig. 9. Membership functions the output K_i^* .

TABLE II. FUZZY SWITCHING LOGIC RULE BASE

	e					
Δe	N		Z		P	
	K_p^*	K_i^*	K_p^*	K_i^*	K_p^*	K_i^*
N	PS	PB	PB	PS	PS	PB
Z	PB	PS	MP	MP	PS	PB
P	PB	PS	PS	PB	PB	PS

IV. SIMULATION RESULTS AND DISCUSSIONS

In order to study the dynamic performance of the DFIG (Doubly-Fed Induction Generator) under variable speed conditions using a vector control technique, a simulation was carried out using Matlab/Simulink. The performance is analyzed first with a PI and fuzzy controller, and then with PI-fuzzy controller. The parameters of the wind turbine with DFIG are given in Table 3.

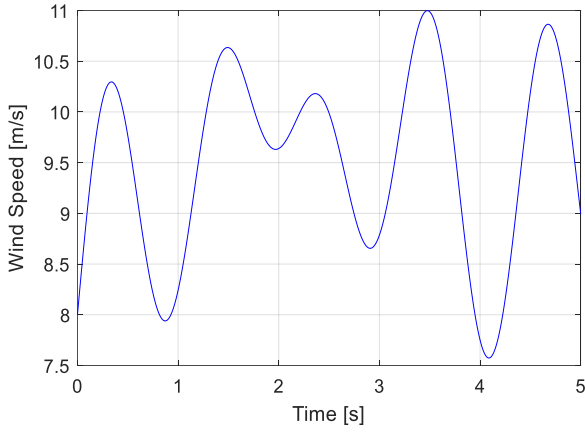


Fig. 10. Wind speed

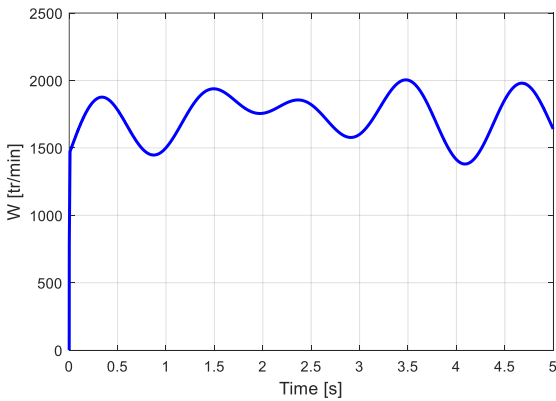


Fig. 11. Mechanical speed.

In the initial test phase, active power generation is directly influenced by wind speed. The stator reactive power is maintained at zero to achieve a unity power factor on the stator side, maximizing the quality of the energy returned to the grid. A mean wind speed of approximately 9 m/s is

applied to the turbine over a 5-second interval. The wind profile used during this simulated period is depicted in Fig 10, while Fig 11 displays the resulting generator speed ω_{mec} (tr/min).

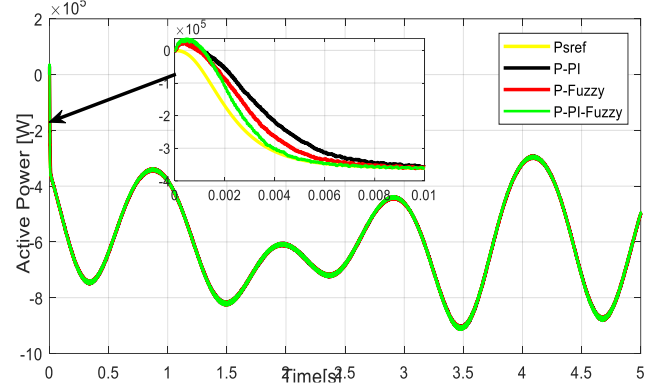


Fig. 12. Active power

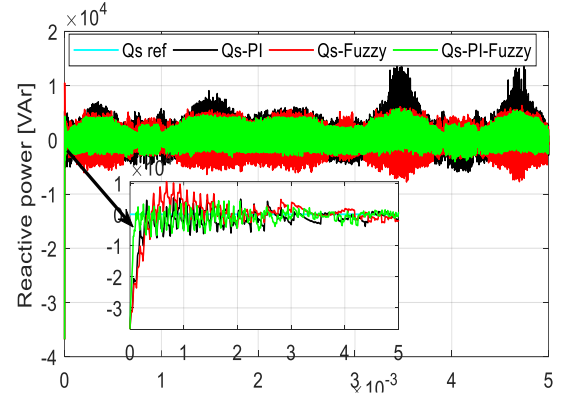
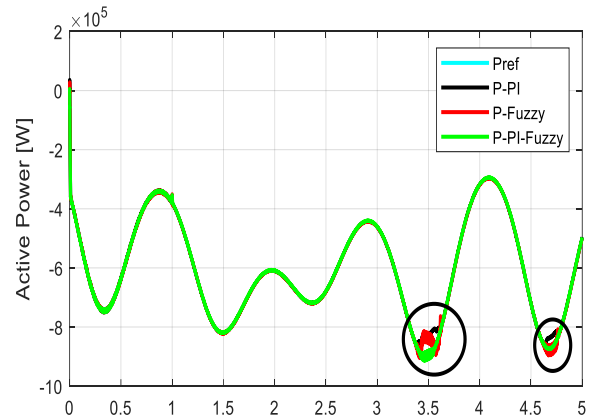


Fig. 13. Réactive power

Fig. 12 and Fig. 13 present the active and reactive power responses for the three control strategies under consideration. The PI-fuzzy controller clearly demonstrates superior performance, exhibiting a faster response time without overshoot, minimal transient oscillations, and accurate tracking of the reference power despite variations in mechanical speed. In contrast, the conventional PI and fuzzy controllers show less desirable characteristics, highlighting the effectiveness of the hybrid PI-fuzzy approach.

Fig. 14. Variation of M (-30%).

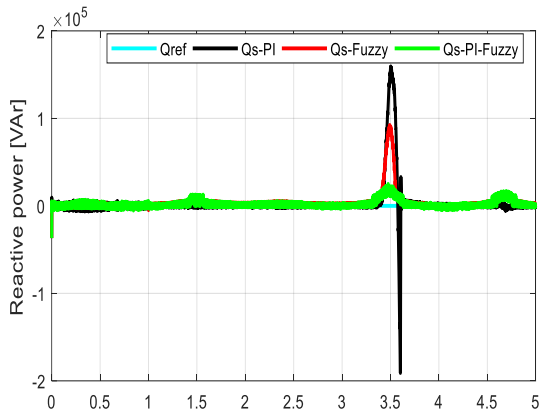


Fig. 15. Variation of M (-30%).

Figures 14 and 15 illustrate the results obtained when varying the mutual inductance. We observe a divergence in the power tracking performance, particularly noticeable with the PI and fuzzy controllers. However, the PI-fuzzy controller consistently demonstrates superior performance and significantly more conclusive results compared to both the standalone PI and fuzzy controllers. This suggests that the combined PI-fuzzy approach offers a more robust and effective control strategy in the face of variations in mutual inductance. The divergence observed in the other controllers may indicate limitations in their ability to adapt to these changes, highlighting the advantage of the hybrid PI-fuzzy approach

TABLE III. DFIG WIND TURBINE PARAMETERS [7]

Parameters	Rated value	Unity
Nominal power P_n	1.5	Mw
Stator voltage V_s	398	V
Stator frequency f_s	50	Hz
Number of pairs poles P	2	
Stator resistance R_s	0.012	Ω
Rotor resistance R_r	0.021	Ω
Stator inductance L_s	0.0137	H
Rotor inductance L_r	0.0136	H
Mutual inductance M	0.0135	H
Gearbox ratio G	90	
Rotor diameter R	35.25	m
Inertia J_t	1000	Kg m ²
Viscous friction F	0.0024	Nm/rad

V. CONCLUSION

This paper details the modeling and proposes a control strategy for a variable-speed wind energy conversion system (WECS) using a doubly-fed induction generator (DFIG). Three types of active and reactive power controllers were developed: a conventional PI and fuzzy controller, and a self-tuning adaptive PI-fuzzy controller. Comparative tests were carried out to evaluate their performance and robustness. The results show that the adaptive PI-fuzzy controller is more efficient and offers better stability and faster convergence towards equilibrium than the conventional PI and fuzzy controller. This performance improvement is attributed to the adaptation of the control gains.

REFERENCES

- [1] N. Choug, S. Benagougne, S. Belkacem, Fuzzy Control with Adaptive Gain of DFIG based WECS, 4th International Conference on Artificial Intelligence in Renewable Energetic Systems IC-AIRES, Alger, Dec. 2020.
- [2] M. Kassa idjdarene: Contribution à L'étude et la Commande de Génératrices Asynchrones à Cage Dédiées à Des centrales Electriques Eoliennes Autonomes, *PHD Thesis, University of Bejaia*, 2010.
- [3] M. Bezza, B.EL. Moussaoui, A. Fakkar, T.I. LEEA: Sensorless MPPT Fuzzy Controller for DFIG Wind Turbine, *Energy Procedia*, 18, 2012, (pp. 339 – 348).
- [4] Y.K. Wu, W.H. Yang: Different Control Strategies on the Rotor Side Converter in DFIG Based Wind Turbines, *Energy Procedia*, 100,2016, (pp. 551 – 555).
- [5] A.R. Solat, A.M. Ranjbar, B. Mozafari: Coordinated control of Doubly Fed Induction Generator Virtual Inertia and Power System Oscillation Damping Using Fuzzy Logic, *International Journal of Engineering*, Vol. 32, No. 4, 2019, (pp. 536 – 547).
- [6] M.F. Iacchetti, G.D. Marques, R. Perini: A scheme for the Power Control in a DFIG Connected to a DC Bus via a Diode Rectifier, *IEEE Transactions on Power Electronics*, Vol. 30, No. 3, 2015, (pp. 1286 – 1296).
- [7] N. Choug : Commande des Entrainements Electriques des Systèmes de Chaîne de Conversion d'Energie Renouvelable, *PHD Thesis, University of Batna 02*, 2021.
- [8] R. Teodorescu, M. Liserre, P. Rodriguez: Grid Converters for Photovoltaic and Wind Power Systems, *West Sussex UK Wiley*, 2011.
- [9] H. Benbouhenni, Z. Benghanem, A. Belaidi: Neuro-Second Order Sliding Mode Control of a DFIG Supplied by a two-Level NSVM Inverter for Wind Turbine System, *Iranian Journal of Electrical and Electronic Engineering*, Vol. 14, No. 4, 2018, (pp. 362 – 373).
- [10] F. Mazouz, S. Belkacem, Y. Harbouche, R. Abdessemed, S. Ouchen, "Active and Reactive Power Control of a DFIG For Variable Speed Wind Energy Conversion", IEEE 6th International conference on systems and control (ICSC'2017), Batna Algeria, 2017, (pp. 173 – 185).
- [11] N. Choug, S. Benagougne, S. Belkacem, Hybrid Fuzzy Reference Signal Tracking Control of a Doubly Fed Induction Generator, *IJE transactions A: Basics*, vVol. 33, No. 4, pp. 567–574, Apr. 2020
- [12] A.A. Sarić, A.Lj. Marjanović: Nonlinear Optimization of Proportional-Integral Controller in Doubly-Fed Induction Generator Using the Gradient Extremum Seeking Algorithm, *Serbian Journal of Electrical Engineering*, Vol. 16, No. 2, 2019, (pp. 161 – 180).
- [13] W. Ayir, H. Ali: Direct Torque Control-Based Power Factor Control of a DFIG, *Energy Procedia*, 162, 2019, (pp. 296 – 305).
- [14] K.M. Nachida: Evaluation du Gisement Energétique Eolien Contribution a la Détermination du Profil Vertical de la Vitesse du Vent en Algérie, *PHD Thesis, University of Tlemcen*, 2006.
- [15] S. Chikha: Active and Reactive Power Management of Wind Farm Based on a Six Leg Tow Stage Matrix Converter Controlled by a Predictive Direct Power Controller, *Iranian Journal of and Electronic Engineering*, Vol. 14, No. 3, 2018, (pp. 245 – 258).

- [16] K. Kerrouche, A. Mezouar, KH. Belgacem: Decoupled Control of Doubly Fed Induction Generator by Vector Control for Wind Energy Conversion System, *Energy Procedia*, 42, 2013, (pp. 239 – 248).
- [17] A.R. Toloei, M. Zarchi, B. Attaran: Optimized Fuzzy Logic for NonLinear Vibration Control of Aircraft Semi - Active Shock Absorber With Input Constraint, *International Journal of Engineering*, Vol. 29, No. 9, 2016, (pp. 1300 – 1306).
- [18] L. Ouada, S. Benaggoune, and S. Belkacem: Neuro-fuzzy Sliding Mode Controller Based on a Brushless Doubly Fed Induction Generator", *International Journal of Engineering (IJE)*, IJE TRANSACTIONS B: Applications Vol. 33, No. 2, 2020, (pp.248–256).
- [19] K. Jash, N. Chakraborty, P.K. Saha, G.K. Panda: Comparative Study Between PI and Fuzzy Logic Speed Controller in Vector Controlled PMSM Drive, *Journal of Engineering Research and Applications*, Vol. 4, No. 4, 2014, (pp. 58 – 62).
- [20] H. Jigang, W. Jie, F. Hui ,An anti-windup self-tuning fuzzy PID controller for speed control of brushless DC motor, *Automatika*, Vol 58, No. 3 , pp. 321–335, 2018.
- [21] H. Chaiyatham, I. Ngamroo, Optimal fuzzy gain scheduling of PID controller Of superconducting magnetic energy storage For power system stabilization, *International Journal of Innovative Computing, Information and Control*, Vol. 9, No. 2 , pp. 651–666, Feb. 2013.
- [22] N. Choug, S. Belkacem, S. Benaggoune , Advanced Direct Torque Control: Employing Fuzzy Logic for Dynamic and Adaptive Regulation, *Journal of Electrical Systems*, Vol 20, No. 3 , pp. 9289 - 9300, 2024.